# Paleozoic geomagnetism shapes vertebrate evolution

**John Phillip Staub**

Unaffiliated researcher
Corresponding Author: John P. Staub Email address: paleopjs@yahoo.com

**Background.** Despite a fifty-year failure of paleontologists to find a viable connection between geomagnetic polarity reversals and evolutionary patterns, recent databases show that the early appearance, radiation, and diversification of Paleozoic vertebrates tends to occur during periods having frequent collapses of the Earth's geomagnetic field. The transition time during the collapse of the Earth's protective magnetic shield can last thousands of years, and the effects on biota are unknown. Solar and cosmic radiation, volcanism, weather alteration, low-frequency electromagnetic fields, depletion of ozone, and the stripping of atmospheric oxygen have been proposed as possible causes, but previous studies have found no effects.

**Methods.** Using published databases, we compiled a spreadsheet that shows the first appearance of 1809 age-dated genera with each genus assigned to one of 28 taxonomic groups. From Gradstein's Geologic Time Scale 2012, we delineated 17 Paleozoic zones with either high or low levels of polarity reversals.

**Results.** From our compilation, we counted 508 Paleozoic vertebrates that first appeared within 20 million-years of the origin of their clade or natural group. These genera represent the initial radiation and diversification of individual Paleozoic vertebrate clades. After compensating for sample-size and external geologic biases, the resulting Pearson's coefficient between these genera and polarity zones equals 0.781. Using 11 commonly accepted clades and assuming a natural competition existed between them, we counted each genus from a clade's inception until it was bypassed by a subsequent clade. Here, Pearson's equals 0.901 with a p-value of <0.000001. In a blindfold study, we separated the Paleozoic into a dozen equally-sized temporal bins, then 13 bins, up to 31 bins. The mean Pearson coefficient for these bins is 0.810. After calculating coefficients for four distinct taxonomies, two paleomagnetic systems, three systematics for age-dating within geologic stages, and seven independent spreadsheets, the results suggest a strong relationship exists between Paleozoic vertebrates and polarity reversals.

In addition, the earliest species of the major divisions of Paleozoic vertebrates (jawless fish, armored fish, jawed fish, cartilage fish, fish with bones, lobe-finned fish, tetrapods, amphibians, reptiles, and synapsids) first appeared in zones with relatively high levels of polarity reversals.

**Discussion.** The question: is this apparent connection between geomagnetism and the evolution of Paleozoic vertebrate due to environmental or biologic factors. If biologic, why are vertebrates the only biota effected? And after an indeterminate period of time, how do vertebrate families become immune to the ongoing effects of polarity reversals?

PeerJ Preprints | https://doi.org/10.7287/peerj.preprints.26490v1 | CC BY 4.0 Open Access | rec: 7 Feb 2018, publ: 7 Feb 2018

## Introduction

Geomagnetic polarity reversals have occurred randomly throughout the Phanerozoic at a rate of two or three times per million years. The transition between the collapse of the Earth's protective magnetic shield and its subsequent regeneration can last thousands of years, and no one knows what the effects on biota during this interim have been in the past or might be in the future. Numerous researchers have searched for answers, both pro and con (Glassmeier, 2010). Uffen first raised the possibility that polarity reversals could increase extinction rates due to harmful solar and cosmic radiation (Uffen, 1963). Others soon pointed out the Earth's atmosphere is our primary shield despite a potential loss of ozone (Crutzen, 1975). Secular variations of a weakening geomagnetic field intensity show enhanced cosmic-ray production of $^{10}$Be and $^{36}$Cl in the stratosphere (McHargue, 2000). Reinforcing this view, age-dated Greenland ice cores show increasing concentrations of $^{10}$Be during polarity excursions (Raisbeck, 2006). Despite active DNA repair mechanisms, all life forms are susceptible to high levels of UV exposure (Glassmeier, 2010). Volcanism (Courtillow, 2007), weather alteration (Harrison, 1974), low-frequency electromagnetic fields (Liboff, 2013), depletion of ozone (Huang, 2017), and the stripping of atmospheric oxygen (Wei, 2014) have been proposed as possible culprits, but Glassmeier and Vogt in their review of *Magnetic Polarity Transitions and Biospheric effects* listed numerous causations but found no evidence of effects (Glassmeier, 2010). Pechersky's study found minimal correlation between biozones and geomagnetic polarity (Pechersky, 2012). And analysis of Sepkoski's 2002 marine fossil compendium shows virtually no alignment of biota and polarity reversals—with one exception, family-level Paleozoic vertebrates.

The Paleozoic is the only geologic era of the Phanerozoic with two polarity superchrons (the Kiaman and Moyero) plus six polarity chrons lasting more than 6 myr. The question: can these polarity chrons be correlated with Paleozoic vertebrates using current taxonomic compilations.

## Methods

The Paleobiology database (paleodb.org) is an ideal source to build a compilation of genus-level Paleozoic vertebrates, but it is not yet fully complete. Therefore, we added Benton's list of terrestrial vertebrates from the supplemental in *The first half of tetrapod evolution* (Benton, 2013), plus data from Zhao and Zhu's *Siluro-Devonian vertebrate biostratigraphy and biogeography of China* (Zhoa, 2009), and Sepkoski's 2002 marine compendium. From these sources, we compiled a spreadsheet that lists the first appearance (FAD) of 1809 genera that are dated by geologic stage as specified by The Geologic Time Scale 2012 (Gradstein, 2012). In addition, each genus was assigned to one of 28 taxonomic groups as defined by Paleobiology or by Benton in the appendix of his book, *Vertebrate Palaeontology* (Benton, 2013). Fossilworks (fossilworks.org) clarified taxon classification when necessary.

We dated 303 individual Paleozoic geomagnetic polarity reversals taken from Gradstein, 2012, Ogg, 2016, Hansma, 2015, Lanci, 2013, Hounslow, 2016, and Opdyke, 2009. From their data, we delineated nine Paleozoic zones with high levels of polarity reversals (HPZ) lasting 130.4 million years (myr), and eight low-level polarity zones (LPZ) lasted 138.4 myr. See Figure 1. Each of the 1809 genera was assigned to a specific polarity zone (see supplemental, Data S1).

PeerJ Preprints | https://doi.org/10.7287/peerj.preprints.26490v1 | CC BY 4.0 Open Access | rec: 7 Feb 2018, publ: 7 Feb 2018

**Figure 1 Polarity Reversals and Distribution of Paleozoic vertebrates.**

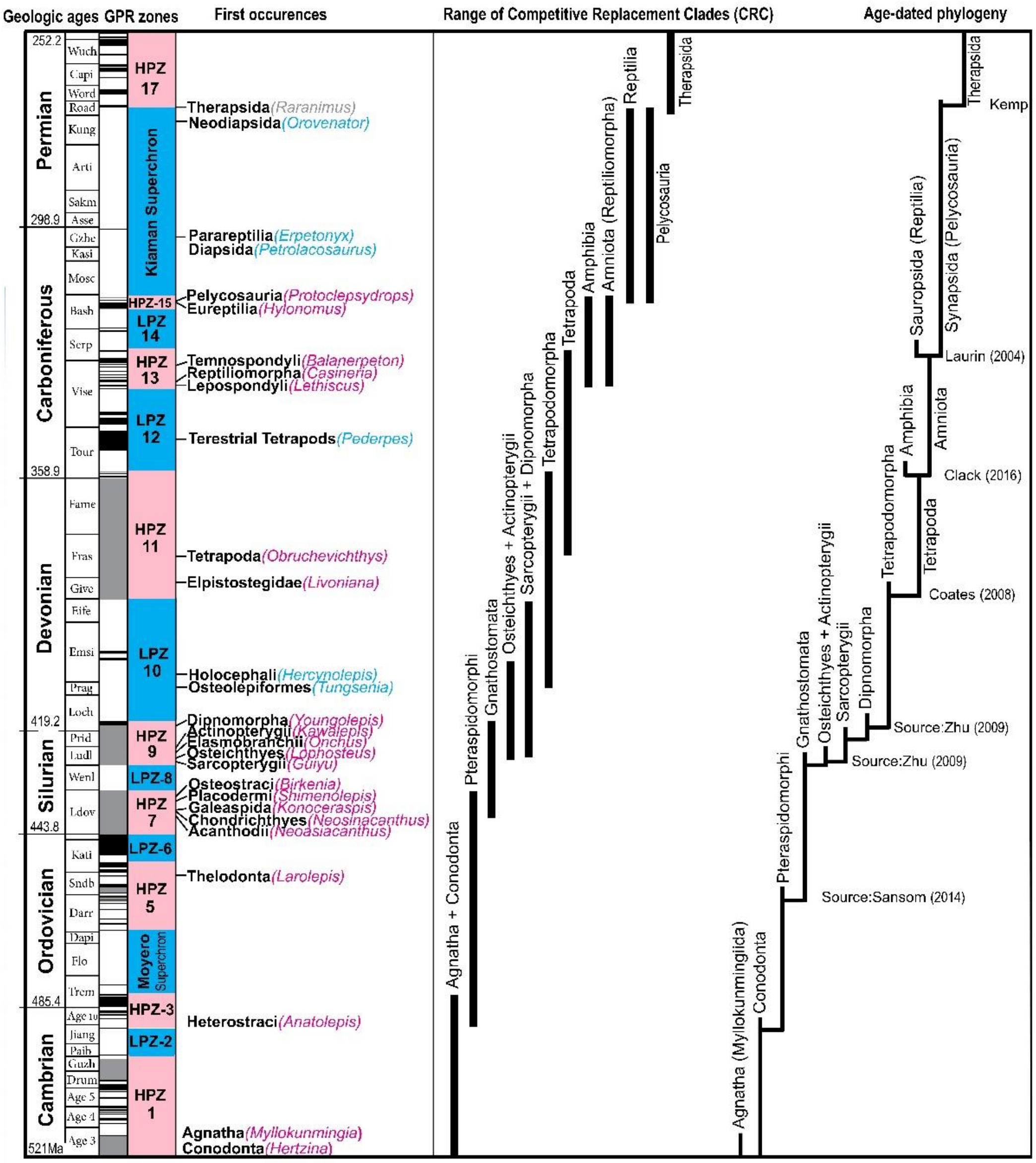

Columns (1) and (2): geologic periods and stages age-dated from Gradstein 2012. Column (3): geomagnetic polarity reversals from multiple sources (black is normal polarity; white is reversed; gray represents multiple reversals). Column (4): high (red) and low polarity (blue) zones. Column (5): FAD of originating genus of 28 clades. Column (6): Ranges of competitive replacement clades (CRC) from their origination until bypassed by a succeeding clade. Column (7): Possible age-dated phylogeny of Paleozoic vertebrates, with sources.

An insignificant 52.9% (958/1809) of the compiled genera originated in high polarity zones. Neither marine fauna at 51.0% (577/1131), nor post-Devonian tetrapods at 56.2%, (678/381) showed significant improvement. Nonetheless, the first appearance of every major divisions of Paleozoic vertebrates (agnathans, conodonts, pteraspidomorphs, gnathostomes, osteichthyans, actinopterygians, sarcopterygians, tetrapods, amphibians, reptiles, and synapsids) occurred in high-polarity zones. Twenty-three of Benton's 28 class-level natural groups and monophyletic clades of vertebrates (82.1%) first appeared in high polarity zones (see Table 1).

We used multiple sources to define the originating species and its FAD of 28 monophyletic and polyphyletic clades (Table 1). The post-origin time of an individual genus is the time in millions of years (myr) after the FAD of the clade's originating genus. We counted all genera with a post-origin time of less than 5 myr, then calculated the percentages of genera originating in high polarity zones compared to the total genera. Likewise, we found the percentages of high-polarity genera with a post-origin time of zero to 10 myr, then 0-15 myr, stepwise up to 50 million years. Figure 2a shows the percentages for the intervals, 0-5 myr through 0-50 myr. Note the percentage falloff after 20 myr.

Now, the question becomes more specific: does the early radiation and diversification of a clade or natural group correlate with polarity reversals?

## Results

From our final compilation of 1809 genera, we counted 508 Paleozoic vertebrates (abbreviated 20G) with a post-origin time of less than 20 million-years. These 20G genera represent the initial radiation and diversification of individual Paleozoic vertebrate clades. 74% of the 508 20G genera are found in high-polarity zones.

Extrinsic biases such as outcrop area and accessibility are known to affect the distribution of fossils (Peters, 2001). Sample-size is a potential problem (for example, we have only five actinopterygians compared to over 200 therapsids). To partially nullify these biases, we simply divided the 20G genera by the total genera within each polarity zone (see Tables 2 and 3), then correlated those percentages to the rate of polarity reversals per million years for each of our 8 high and 7 low polarity zones. The resulting Pearson's correlation coefficient equals 0.674 with a p-value of .00303. After correcting for the Cambrian problem (see calculations section), Pearson's equals 0.781 with a p-value of .0003.

The 20G vertebrates represent the original diversification and radiation of vertebrate clades. They are defined as all genera found within a twenty-million period after the FAD of the originating fossil of each clade, but new discoveries can alter those dates, and the twenty-million-year cutoff, although statistically significant, is obviously arbitrary. Nor will Benton's—or anyone's—choice of clades be universally accepted. In reality, reclassification of a single genus might disrupt the 20G statistical results.

A more reliable and simplified system is to replace the 28 clades with only 11 commonly-accepted major groups, and assume a natural competition exists between them. The Early Cambrian 'agnathans' (including conodonts) are counted as positive until the first appearance of the pteraspidomorphs with their protective scales and armor; the jawless fish until the gnathostomes; the jawed fish until the osteichthyans; the bony fish until the sarcopterygians; the lobe-finned fish until the tetrapodomorphs; the tetrapodomorphs until the Upper Devonian tetrapods; the early tetrapods until the amphibians; the temnospondyls and lepospondyls until the amniotes; the reptiles and pelycosaurs until the therapsids. We counted each genus from a clade's inception until it was bypassed by a subsequent clade. 538 Paleozoic genera were assigned as positive to these competitive replacement clades (CRC). 397 of the CRC genera (73.8%) are found in high-polarity zones. Pearson's correlation equals 0.691 with a p-value of .00215. After correcting for the Cambrian problem (see calculations section), Pearson's equals 0.901 with a p-value of <0.000001.

Choosing the boundary of a paleomagnetic zones is somewhat arbitrary, and so in a blindfold study, we separated the Paleozoic into a dozen equally-sized temporal bins (<12 bins are statistically insignificant). For each bin, we counted the CRC genera, total genera, and number of polarity reversals, then we compared the polarity reversals to the CRC genera divided by the total genera within each bin. Pearson's correlation equals *0*.846. We also separated the Paleozoic into 13 bins (Pearson's rho=0.865), then 14 bins (Pearson's=*0*.864), and up to 30 equally-sized bins. For 15 bins, *r*=0.831.; 16 bins, *r*=0.839; 17 bins, *r*=0.847; 18 bins, *r*=0.847; 19 bins, *r*=0.834; 20 bins, *r*=0.785; 21 bins, *r*=0.792; 22 bins, *r*=0784.; 23 bins, *r*=0.731; 24 bins, *r*=0.786; 25 bins, *r*=0.813; 26 bins, *r*=0.791; 27 bins, *r*=0.83; 28 bins, *r*=0.818; 29 bins, *r*=0.738; 30 bins, *r*=0.741. For CRC genera, the mean Pearson's correlation coefficient for these 19 bins is 0.810. For 20G genera, the mean Pearson's correlation is 0.602. No corrections were made for the Cambrian genera when calculating bins.

It is apparent that Paleozoic vertebrates originated and radiated in alignment with polarity reversals. Each of the 10 major divisions of Paleozoic vertebrates first appear in a high-polarity zone. Table 4 shows correlation coefficients and p-values for four taxonomies (Paleobiology's, Benton's classification, a final composite system, and the competitive replacement clades); two paleomagnetic references (Gradstein, 2012, et al. and Ogg, 2016); occurrences vs. total genera; basal, median, and proportional dating of geologic stages; 20G and CDC genera with seven independent spreadsheets (see the Detailed Methodology section for a description of the seven spreadsheets). After correcting for the Cambrian problem, the CRC genera have an average p-value of <0.001 (highly significant); half of the 20G systems are <0.001 (highly significant) and the other half, <0.05 (significant). These results, shown in Table 4, strongly suggest a relationship exists between Paleozoic vertebrates and geomagnetic polarity reversals.

**Table 1 | FAD of earliest known species of Paleozoic clades** (reds are high-polarity zones).

| Major Clades | Genus | Geologic stage | Range | Median | Zone | Source |
|---|---|---|---|---|---|---|
| Synapsida (Pelycosauria) | Protoclepsydrops | Westphalian A | 318.6-317.8 | 318.2 | HPZ-15 | Paleobiology |
| Reptilia (Eureptilia) | Hylonomus | Westphalian A | 318.6-317.8 | 318.2 | HPZ-15 | Paleobiology |
| Amniota (Reptiliomorpha) | Casineria | Asbian | 336.5-332 | 334.2 | HPZ-13 | Paleobiology; See Note 1 |
| Amphibia (Lepospondyli) | Lethiscus | Early Asbian | 336.5-334.2 | 335.4 | HPZ-13 | See Note 1 |
| Tetrapoda | Obruchevichthys | Frasnian | 382.7-372.2 | 377.4 | HPZ-11 | Paleobiology |
| Osteichthyes | Lophosteus | Late Gorstian | 426.5-425.6 | 426 | HPZ-9 | Sepkoski |
| Sarcopterygii | Guiyu | Gorstian | 427.4-425.6 | 426.5 | HPZ-9 | Zhoa & Zhu |
| Gnathostomata (Placodermi) | Shimenolepis | Middle Telychian | 436.8-435.1 | 436 | HPZ-7 | Zhoa & Zhu |
| Pteraspidomorphi | Anatolepis | Sunwaptan, Mid | 490.8-488.5 | 489.6 | HPZ-3 | Smith (2007); see Note 4 |
| Agnatha | Myllokunmingia | Atdabanian | 521-516.1 | 518.6 | HPZ-1 | Paleobiology |
| **Benton's Clades** | | | | | | |
| Lepidosauromorpha | Lacertulus | Early Wuchiapingian | 259.8-257 | 258.4 | HPZ-17 | Paleobiology |
| Archosauromorpha | Eorasaurus | Capitanian | 265.1-254.2 | 259.7 | HPZ-17 | Paleobiology |
| Neodiapsida | Orovenator | Kungurian | 279.3-272.3 | 272.3 | LPZ-16 | Paleobiology |
| Parareptilia | Erpetonyx | Gzhelian | 303.7-298.9 | 301.3 | LPZ-16 | Paleobiology |
| Diapsida | Petrolacosaurus | Missourian | 306-303.7 | 304.8 | LPZ-16 | Paleobiology |
| Batrachomorpha (Temnospondyli) | Balanerpeton | Early Brigantian | 332-331.4 | 331.7 | HPZ-13 | Paleobiology w/Stratcomments |
| Tetrapodomorpha | Tungsenia | Late Pragian | 409.2-407.6 | 408.4 | LPZ-10 | Lu (2012); see Note 2 |
| Chondrichthyes(Subterbranchialia) | Petalodus | Famennian | 372.2-358.9 | 365.5 | HPZ-11 | Zhoa & Zhu |
| Chondrichthyes (Holocephali) | Hercynolepis | Early Emsian | 407.6-400.4 | 404 | LPZ-10 | Zhoa & Zhu |
| Dipnomorpha | Youngolepis | Early Lochkovian | 419.2-416.4 | 417.8 | HPZ-9 | Zhoa & Zhu |
| Actinopterygii | Kawalepis | Late Ludfordian | 424.3-423 | 423.6 | HPZ-9 | Zhoa & Zhu |
| Actinopteri | Ligulalepis | Late Ludfordian | 424.3-423 | 423.6 | HPZ-9 | Zhoa & Zhu |
| Chondrichthyes (Elasmobranchii) | Onchus | Ludfordian | 425.6-423 | 424.3 | HPZ-9 | Paleobiology |
| Osteostraci | Birkenia | Late Llandovery | 438.6-430.4 | 434.5 | HPZ-7 | Paleobiology w/Stratcomments |
| Chondrichthyes | Neosinacanthus | Early Telychian | 438.5-436.8 | 437.6 | HPZ-7 | Zhu (1998); see Note 3 |
| Acanthodii | Neoasiacanthus | Early Telychian | 438.5-436.8 | 437.6 | HPZ-7 | Zhu (1998); see Note 3 |
| Galeaspida | Konoceraspis | Early Telychian | 438.5-436.8 | 437.6 | HPZ-7 | Zhoa & Zhu |
| Chordata (Conodonta) | Hertzina | Nemakit-Daldynian | 530.7-525.3 | 528 | HPZ-1 | Paleobiology |
| **Additional Clades** | | | | | | |
| Synapsida (Therapsida) | Raranimus | Mid-late Roadian | 271.7-268.8 | 269.95 | LPZ-16 | see note 5 |
| Carboniferous Tetrapoda | Pederpes | Ivorian | 351.3-346.7 | 349 | LPZ-12 | Paleobiology |
| Elpistostegidae | Livoniana | Late Givetian | 384.37-382.7 | 383.535 | HPZ-11 | Paleobiology |
| Thelodonta | Larolepis | Franklinian | 460.9-449.5 | 455.2 | HPZ-5 | Paleobiology |

Note 1: *Casineria* (Cheese Bay Shrimp Bed) and *Lethiscus* (Wardie Shales) were discovered in the *Perotrilites tessellatus/Schulzospora campyloptera* microspore zone (Late Holkerian to Early Asbian). *Casineria* is listed as Asbian. Wardie Shales were deposited slightly before the Cheese Bay Shrimp, thus *Lethiscus* is Early Asbian (VanTuinen, 2004; Paton, 1999). Note 2: *Tungsenia* is the earliest known tetrapodamorph (Lu, 2012). Note 3: *Neoasiacanthus* is an acanthodian, based on the number of ridges on the fin spines (Zhu, 1998). Note 4: *Anatolepis* is a pteraspidomorph. Note 5: *Raranimus* replaces *Tetraceratops* as the earliest therapsid. It is improbable that Raranimus, is Early Roadian (Kemp 2006; Liu 2009). Li equates Raranimus to Zone II in Russia which is likely Middle Roadian (Liu, 2001,2009).

**Figure 2**

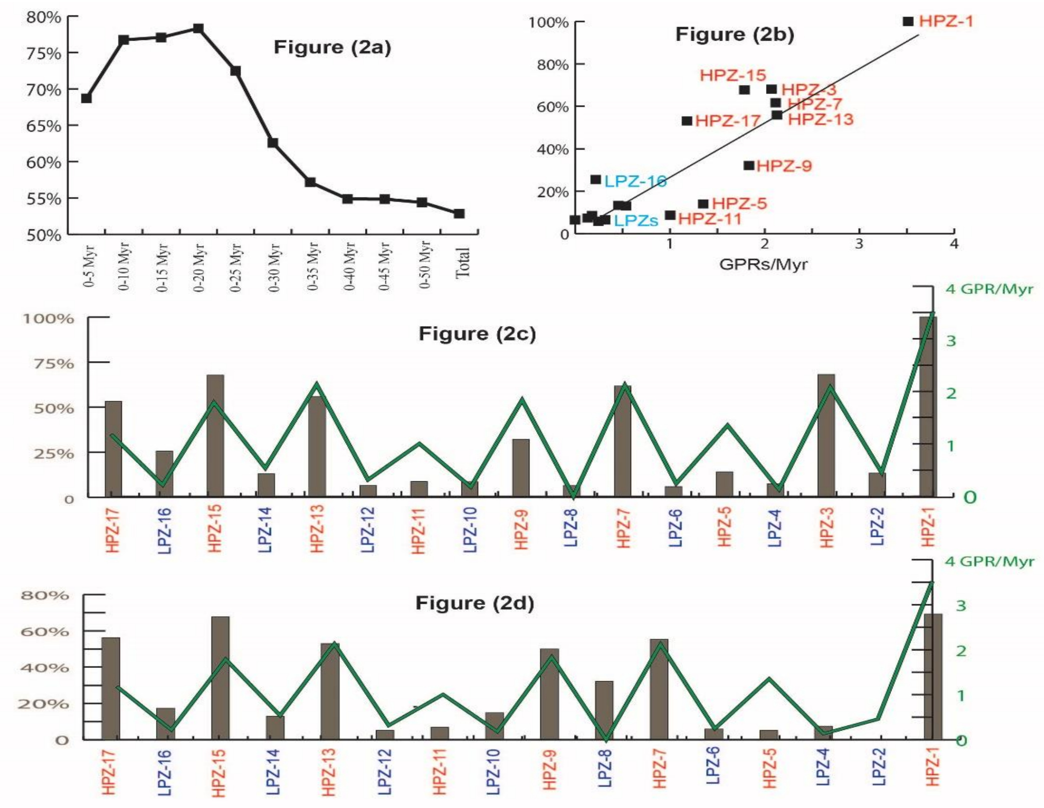

**Figure 2a** shows percentages of Paleozoic vertebrate genera discovered in high-polarity zones relative to the total genera from 0-5, 0-10 myr, to 0-50 myr. Note the falloff after 20 myr. 'Total' is the percentage for all 1809 genera.

**Figure 2b** is a scatter plot of polarity zones comparing the reversals per myr to the CRC genera divided by the total genera within each zone. The CRC (competitive replacement clades) are active clades early in their diversification until bypassed by a more-successful clade. Reds are high-polarity zones; blues are low-polarity zones.

**Figure 2c** is the bar graph of the CRC genera (the zigzag lines are polarity reversals per myr). HPZ-1 has a percentage of 100% which may be too high, but it is balanced by HPZ-11 where the number of marine tetrapods is low compared to the large numbers of Devonian fish.

**Figure 2d** is the bar graph for 20G genera. The earliest genera of a clade represents the initial radiation of that clade. The 20G genera are all genera with a post-origin time of less than 20 myr following the original FAD of the earliest species of that clade. For example: *Guiyu*, the originating sarcopterygian, was discovered in the Gorstian Stage of the Upper Silurian which is dated at 427.4 to 425.6 Ma (median age is 426.50 Ma). *Porolepis* is date at 404.03 Ma. Therefore, *Porolepis* has a post-origin time of 22.47 myr, median age. Note that HPZ-3 is void of all species and was eliminated (see Calculations Section).

## Discussion

Although the statistical evidence connects the fossil record of Paleozoic vertebrates to polarity reversals, it does not determine if the causation is extrinsic (geologic) or intrinsic (biologic). Nor does it answer a larger question: Do polarity reversals directly affect vertebrate evolution due to increasing mutation rates?

Fossilization is dependent on positive environmental conditions such as rapid burial or anoxia. Poor environmental conditions can cause gaps in the fossil record. Romer's Gap (LPZ-12) of the Early Carboniferous is now thought to be a sampling artifact (Anderson, 2015; Clack, 2016), but other gaps exist. The Middle Carboniferous Namurian Stage (LPZ-14) has been called a gap in the tetrapod record (Clack, 2012). Olsen's gap runs between the last occurrence of pelycosaurs in North America until the earliest appearance of therapsids in the uppermost Kiaman superchron (LPZ-16). The Moyero Superchron (LPZ-4), shows active diversification of conodonts but limited signs of agnathan vertebrates. The Cambrian Paibian/Jiangshanian (LPZ-2) gap has only two originating conodonts, while the Upper Ordovician LPZ-6 is void of any vertebrates other than conodonts. That these gaps correlate with low-polarity zones implies the causation is environmental, not biologic.

The first appearance of a genus is not the origin of the species, and ghost lineages can be extensive. Age-dated phylogenies, dependent on molecular or morphological variation, attempt to date the origin, but phylogenetic analysis is often impaired by a lack of articulated fossils—and parsimony is never a grantor of accuracy. Worse, results are prone to differing opinions or new discoveries. The amniote/amphibian divergence is now placed in the earliest Carboniferous (HPZ-11)(Clack, 2016). *If* this phylogeny is confirmed, and *if* Zhu's minimal phylogenetic dates for the osteichthyans, actinopterygians, sarcopterygians, dipnomorphs, and tetrapodomorphs are upheld (Zhu, 2009), and *if* the earliest pteraspidomorph is dated no more than a million years prior to the single scale of *Anatolepis* that was discovered in the Middle Sunwaptan (multiple scales were found in the Upper Sunwaptan)(Smith, 2007), and *if* limb-bearing tetrapods originated in the Late Devonian (Coates, 2008), and assuming the Polish tetrapod trackways are actually fish nests or feeding traces (Lucas, 2015), and *if* Laurin's estimated synapsid/sauropsids node is correct (Laurin, 2004) and *if* the true identity of the poorly preserved and fragmented early Kazanian Russian fossils are not therapsids (Kemp, 2006), then it's *not impossible* that every major clade of Paleozoic vertebrates originated in a high-polarity zone, and *if so*, the causation for the connection between polarity reversals and vertebrates would be biologic, not environmental.

Volcanic activity, weather alteration, and the depletion of ozone have been linked to geomagnetic polarity reversals. But if these external causations are the connection between Paleozoic vertebrate evolution and geomagnetism, then why are only vertebrates affected? Why not invertebrates? And after an indeterminant period of time (we used 20 myr), how do vertebrate families become immune to the ongoing effects of polarity reversals? Are DNA repair mechanisms involved?

PeerJ Preprints | https://doi.org/10.7287/peerj.preprints.26490v1 | CC BY 4.0 Open Access | rec: 7 Feb 2018, publ: 7 Feb 2018

In reality, any usage of taxonomic group might be considered faulty. Evolution is a continuum with natural groups and clades merely artificial tools useful for clarification. Nonetheless, the continuum of evolution does not keep mutation rates from increasing periodically, nor does it keep the pace of evolution from accelerating during geomagnetic polarity collapses.

## Detailed Methodology

### Generating the seven Paleozoic compilations

Originally, we compiled a list of over 2000 Paleozoic vertebrate genera taken from multiple sources, but this early compilation lacked repeatability. Therefore, we limited our sources to the Paleobiology Database (Feb 9, 2017, upgraded Sept 17, 2017), Sepkoski's 2002 marine compilation, Benton's 2013 compilation in *The first half of tetrapod evolution*, plus Zhao and Zhu's 2010 *Siluro-Devonian vertebrate biostratigraphy and biogeography of China*. A single source would be ideal, but the Paleobiology Database lacks many marine and terrestrial vertebrates, and their Phylum/Class/Order/Family taxonomy is often inadequate. We used Gradstein 2012 to date the geologic stages, and Paleobiology's "stratcomments" column for precise dating. Any genus, imprecisely dated at >20 myr, was removed. Fossilworks was referenced when necessary, but any genus not listed by the four main sources was ignored for statistical analysis. Duplicate genera often occurred with our four sources. If so, Sepkoski had low priority. Otherwise, we chose the earliest, most precise date.

For our first four spreadsheets, the clades and natural groups were defined by the four original compilations. For variation, we switched to Benton's classification of vertebrate classes from the appendix of his book, *Vertebrate Palaeontology*. For our final composite compilation, we reinstalled the Thelodonts and Osteostraci, and separated the four Elpistostegidae genera from the "tetrapodomorphs". The tetrapods were divided into Upper Devonian marine genera and Carboniferous tetrapods. We combined Lepidosauromorpha and Archosauromorpha within Neodiapsida, and switched *Tetraceratops* and *Dimacrodon* from therapsids to pelycosaurs.

But any complete, balanced, accurate, and impartial Paleozoic compilation from whatever source, should reach equivalent conclusions.

### Generating Geomagnetic Polarity Zones

Gradstein and Ogg 20122, with updated data from Hansma[18], Lanci[19], Hounslow[20], Ogg 201617 and Opdyke[21], was used to individually date 303 Paleozoic geomagnetic polarity reversals and to define 9 high-level and 8 low-level polarity zones. Post-Cambrian, 193 polarity reversals occurred in 233.4 million years (0.827 polarity reversals per million years). This 0.827 value was used as a guide to delineate polarity zones. We extended the high-polarity zones by .2 myr after the uppermost polarity reversal in a zone (excluding the Silurian). The high-polarity zones equal 130.4 myr; the low-polarity zones equal 138.4 myr. See a list of individual polarity reversals below.

PeerJ Preprints | https://doi.org/10.7287/peerj.preprints.26490v1 | CC BY 4.0 Open Access | rec: 7 Feb 2018, publ: 7 Feb 2018

Lanci’s used zircons in his 2013 report on the *Upper Permian magnetic stratigraphy of the lower Beaufort Group in the Karoo Basin of South Africa* to accurately date the base of the Illawara polarity zone (top of the Kiaman superchron) at ~270 mya. He correlates his N3 polarity chron with the Wordian normal, which would place the Eodicynodon AZ into the middle or late Capitanian. It seems more likely, the N3 is an outlier of the Upper Permian Illawarra superchron and should be placed in the Roadian. This has minor effect on our statistics, but potentially could help explain the explosive origin of the therapsids (Kemp, 2005, 2006, 2012) and their possible connection to polarity reversals.

Polarity reversals of post-Jurassic profiles taken from seafloor studies are highly reliable, but Paleozoic geomagnetism needs multiple sites from around the world, and future studies could alter these 17 polarity zones.

## Statistical analysis

The basal age or median age of a geologic stage can be used to date fossils, but geologic stages are often split by polarity zones. For example, the Lochkovian, lasting from 419.2 to 410.8 Ma, is split by the contact of HPZ-9 and LPZ-10 at 416.5 Ma. Only 32% of the Lochkovian is in a high-polarity zone, but when the basal date is used for calculations, 100% of the 41 Lochkovian genera fall into HPZ-9 (zero percent when the median age is used). To solve this problem, we proportionally divided the Lochkovian, and put 28 genera in LPZ-10 and 13 genera in HPZ-9. This way, when only two genera are in a geologic stage or sub-stage, one is placed at the upper two thirds; the other, at the lower third. Proportionality is our preferred dating systematic.

The Cambrian presents a unique problem. There are 13 genera in the Early Cambrian HPZ-1, followed by 2 genera in LPZ-2, and 32 in the Late Cambrian HPZ-3 (See Table 2). This distribution is positive to our hypothesis, but when we divide the two 20G genera by the total of two genera in LPZ-2, the results equal 100%. To compensate, we add the 13 genera from HPZ-1 to the two genera from LPZ-2 and use 15 as the total genera in LPZ-2, lowering the percentage from 100% to a more reasonable 12.5%. Likewise, for HPZ-3, the 32 genera are divided by the total of 47 (13+2+32=47). For 20G genera, the conodonts in HPZ-3 extend past their 20 million-year cutoff leaving a void, and to compensate, we delete HPZ-3 (see Table B and Figure 2d).

A potential problem to this hypothesis: if the FAD of every originating genus first appeared at the base of a high-polarity zone that lasted exactly 20 million-years, then 100% of the 20G genera would be found in high-polarity zones. In reality, the total possible years for our 28 clades is 560 myr with 283.92 myr in high-polarity zones (50.7%).

To calculate equal-sized polarity bins, the post-Terreneuvian Paleozoic lasted for 268.8 myr (521 to 252.2 myr). Therefore, for 20 bins, each bin equals 13.44 myr. Excel automatically counts the total number of genera, the total number of 20G or CRC genera, and the number of polarity reversals for any number of bins, 12 to 31. No corrections for the Cambrian genera are made when calculating bins.

**Table 2 | Geomagnetic polarity zones and Total Distribution of Paleozoic Vertebrates.** Tables 2 and 3 are combined to calculate coefficients with results in Table 4.

| Polarity Zones | | Duration | | Reversals | | Total Distribution | | | Occurrences | |
|---|---|---|---|---|---|---|---|---|---|---|
| **Zone (a)** | **Geologic stages (b)** | **Ma (c )** | **Myr (d)** | **GPRs** | **perMyr** | **Proportion** | **Basal** | **Mid(i)** | **Basal** | **Mid(k)** |
| HPZ-17 | Late Permian | 270-252.2 | 17.8 | 21 | **1.18** | 415 | 395 | 411 | 1464 | 1534 |
| LPZ-16 | Kiaman Superchron | 316-270 | 46 | 10 | **0.22** | 403 | 415 | 403 | 2162 | 2118 |
| HPZ-15 | Westphalian A & B | 318.8-316 | 2.8 | 5 | **1.79** | 31 | 24 | 32 | 133 | 106 |
| LPZ-14 | Late Serpkhovian-Early Bashkirian | 328.1-318.8 | 9.3 | 5 | **0.54** | 46 | 58 | 48 | 237 | 266 |
| HPZ-13 | Late Visean | 337.5-328.1 | 9.4 | 20 | **2.13** | 35 | 37 | 33 | 89 | 81 |
| LPZ-12 | Romer's Gap | 356.5-337.5 | 19 | 6 | **0.32** | 76 | 57 | 80 | 321 | 691 |
| HPZ-11 | Late Devonian | 388.4-356.5 | 31.9 | 32 | **1.00** | 219 | 237 | 214 | 4784 | 4429 |
| LPZ-10 | Middle Devonian | 416.5-388.4 | 28.1 | 5 | **0.18** | 222 | 193 | 239 | 2380 | 3788 |
| HPZ-9 | Late Silurian-Early Lochkovian | 427.4-416.5 | 10.9 | 20 | **1.83** | 106 | 138 | 92 | 3393 | 1958 |
| LPZ-8 | Wenlock Stage | 433.4-427.4 | 6 | 0 | **0.00** | 31 | 31 | 31 | 2894 | 2889 |
| HPZ-7 | Early Silurian | 443.8-433.4 | 10.4 | 22 | **2.12** | 47 | 48 | 48 | 1166 | 1174 |
| LPZ-6 | Katian | 452-443.8 | 8.2 | 2 | **0.24** | 17 | 14 | 15 | 528 | 877 |
| HPZ-5 | Middle Ordovician | 466.8-452 | 14.8 | 20 | **1.35** | 57 | 52 | 57 | 1304 | 1070 |
| LPZ-4 | Moyero Superchron | 482-466.8 | 15.2 | 2 | **0.13** | 54 | 47 | 67 | 707 | 1031 |
| HPZ-3 | Age 10, Late Cambrian | 490.2-482 | 8.2 | 17 | **2.07** | 32 | 46 | 21 | 561 | 98 |
| LPZ-2 | Early Furongian | 496.8-490.2 | 6.6 | 3 | **0.45** | 2 | 1 | 2 | 68 | 77 |
| HPZ-1 | Early Cambrian | 521-496.8 | 24.2 | 85 | **3.51** | 13 | 15 | 13 | 85 | 85 |

Table 2 shows the 17 high (red) and low polarity zones (blue), their range (Ma), duration (myr), number of polarity reversals, reversals per million years, and distribution of total genera in each polarity zone using the median age, basal age, and proportional age of geologic stages used in this compilation. The distribution of genera is generated from our seven Excel spreadsheets can be found in the supplemental, Data S1. Occurrences are taken from the count of total Paleozoic genera in the Paleobiology database.

PeerJ Preprints | https://doi.org/10.7287/peerj.preprints.26490v1 | CC BY 4.0 Open Access | rec: 7 Feb 2018, publ: 7 Feb 2018

**Table 3 | Distribution of Paleozoic vertebrate genera from individual spreadsheets.**

| Polarity zones (a) | 20G genera (initial radiation) | | | | | | | | CRC genra (competitive replacement) | | | | | | | | | |
|---|---|---|---|---|---|---|---|---|---|---|---|---|---|---|---|---|---|---|
| | Proportional dating of geologic stages | | | | | | | | | | | | | | | | Mid | Base |
| | GPRs from Gradstein, et al. | | | | | | | Ogg (2016 | | GPRs from Gradstein, et al. | | | | | | | | |
| | Paleobiolog.org (b) | plus Sepkoski's compilation | plus Benton's compilation | plus Zhoa & Zhu (e) | Corrected dating (f) | Benton's classification | Final Taxonomy (h) | Final Taxonomy (i) | Final Taxonomy (j) | Paleobiolog.org (k) | plus Sepkoski's compilation | plus Benton's compilation | plus Zhoa & Zhu (n) | Corrected dating (o) | Benton's classification | Final Taxonomy (q) | Final Taxonomy (r ) | Final Taxonomy (s) |
| HPZ-17 | 135 | 235 | 235 | 234 | 234 | 233 | 233 | 221 | 207 | 124 | 126 | 219 | 221 | 220 | 221 | 220 | 219 | 214 |
| LPZ-16 | 63 | 72 | 72 | 71 | 71 | 70 | 70 | 80 | 116 | 95 | 94 | 102 | 100 | 104 | 104 | 103 | 104 | 109 |
| HPZ-15 | 12 | 20 | 20 | 21 | 21 | 21 | 21 | 24 | 22 | 12 | 12 | 20 | 20 | 21 | 21 | 21 | 22 | 13 |
| LPZ-14 | 2 | 6 | 6 | 6 | 6 | 6 | 6 | 5 | 5 | 2 | 2 | 6 | 6 | 6 | 6 | 6 | 5 | 12 |
| HPZ-13 | 7 | 11 | 11 | 13 | 13 | 18 | 18 | 17 | 18 | 13 | 13 | 17 | 17 | 19 | 19 | 19 | 18 | 20 |
| LPZ-12 | 1 | 2 | 2 | 0 | 1 | 4 | 4 | 5 | 6 | 2 | 2 | 6 | 6 | 4 | 5 | 5 | 6 | 5 |
| HPZ-11 | 7 | 14 | 14 | 14 | 12 | 15 | 15 | 15 | 19 | 7 | 7 | 13 | 14 | 14 | 20 | 19 | 19 | 20 |
| LPZ-10 | 26 | 32 | 28 | 27 | 33 | 33 | 33 | 35 | 20 | 8 | 10 | 11 | 20 | 20 | 20 | 19 | 23 | 19 |
| HPZ-9 | 21 | 39 | 52 | 53 | 53 | 53 | 53 | 51 | 33 | 12 | 24 | 24 | 33 | 34 | 34 | 34 | 30 | 34 |
| LPZ-8 | 6 | 9 | 11 | 10 | 10 | 10 | 10 | 10 | 2 | 0 | 0 | 0 | 2 | 2 | 2 | 2 | 2 | 2 |
| HPZ-7 | 6 | 6 | 27 | 27 | 22 | 26 | 26 | 26 | 29 | 8 | 8 | 8 | 29 | 29 | 29 | 29 | 29 | 29 |
| LPZ-6 | 1 | 1 | 1 | 1 | 0 | 1 | 1 | 1 | 1 | 1 | 1 | 1 | 1 | 1 | 1 | 1 | 0 | 0 |
| HPZ-5 | 3 | 3 | 3 | 3 | 1 | 3 | 3 | 2 | 5 | 7 | 9 | 9 | 9 | 8 | 8 | 8 | 9 | 9 |
| LPZ-4 | 3 | 4 | 4 | 4 | 4 | 4 | 4 | 5 | 7 | 3 | 4 | 4 | 4 | 4 | 4 | 4 | 15 | 4 |
| HPZ-3 | 0 | 0 | 0 | 1 | 1 | 1 | 1 | 1 | 32 | 27 | 28 | 28 | 28 | 32 | 32 | 32 | 21 | 31 |
| LPZ-2 | 0 | 0 | 0 | 0 | 0 | 0 | 0 | 0 | 2 | 2 | 2 | 2 | 2 | 2 | 2 | 2 | 2 | 1 |
| HPZ-1 | 9 | 9 | 9 | 9 | 9 | 9 | 9 | 13 | 13 | 13 | 13 | 13 | 13 | 13 | 13 | 13 | 13 | 15 |

Table 3 shows the distribution of individual 20G and CRC genera placed in 17 polarity zones using proportional, median, and basal dates. Geomagnetic polarity reversal (GPRs) determine the boundaries of polarity zones. Polarity reversals from Gradstein (2012) with updates from Hansma, Lanci, Hounslow, Ogg 2016 and Opdyke are detailed, but Ogg (2016) is easier to compile. The distribution of genera is taken from our seven spreadsheets found in the supplemental, Data S1. The first spreadsheet is Paleobiology only; the 2nd adds Sepkoski; the 3rd adds Benton's terrestrial vertebrates; the 4th adds data from China; the 5th uses Stratcomments from Paleobiology; the 6th uses Benton's phylogeny; the 7th is a compilation. The yellow rows of the Cambrian zones negatively disrupt the statistical results. For example, the two genera in LPZ-2 when divided by the total distribution from LPZ-2 in Table 2 equals 100%.

**Table 4 Pearson's coefficient calculations and p-values taken from data in Table 1 and Table 2** (The red results, due to the Cambrian statistical anomaly are relatively poor; Dark greens are highly significant).

| Phylogenetic systems | Geomagnetic polarity | Dating systems | Spreadsheets | Pearson (uncorrected) | p-value (uncorrected) | Corrected Pearson's | Corrected p-values | Corrections |
|---|---|---|---|---|---|---|---|---|
| 20G genera | Gradstein's GPRs | Proportional dating | Paleobioloyg.org | 0.6387 | 0.005779 | 0.7361 | 0.001149 | HPZ-3 is deleted |
| | | | plus Sepkoski's compilation | 0.5993 | 0.011003 | 0.7014 | 0.002464 | |
| | | | plus Benton's compilation | 0.5535 | 0.021177 | 0.6563 | 0.005759 | |
| | | | plus Zhoa & Zhu | 0.6266 | 0.007107 | 0.7414 | 0.001011 | |
| | | | Corrected dating | 0.66 | 0.004094 | 0.7618 | 0.000605 | |
| | | | Benton's classification | 0.6445 | 0.005224 | 0.742 | 0.000999 | |
| | | | Final taxonomy | 0.6736 | 0.003033 | 0.7812 | 0.000352 | |
| | Ogg (2016) | | Final taxonomy | 0.7225 | 0.00105 | 0.7057 | 0.0016 | Cambrian percentages are corrected |
| CRC genera | | | Final taxonomy | 0.5236 | 0.031 | 0.764 | 0.000357 | |
| | Gradstein's GPRs | | Paleobioloyg.org | 0.5628 | 0.01866 | 0.8236 | 0.000048 | |
| | | | plus Sepkoski's compilation | 0.5824 | 0.014163 | 0.8483 | 0.000017 | |
| | | | plus Benton's compilation | 0.6025 | 0.010482 | 0.8218 | 0.000052 | |
| | | | plus Zhoa & Zhu | 0.6836 | 0.00248 | 0.8988 | 0.0000009 | |
| | | | Corrected dating | 0.6884 | 0.002246 | 0.8978 | 0.000001 | |
| | | | Benton's classification | 0.6903 | 0.002162 | 0.901 | 0.0000008 | |
| | | | Final taxonomy | 0.6905 | 0.00215 | 0.9014 | 0.0000008 | |
| | | Mid | Final taxonomy | 0.6798 | 0.002682 | 0.8873 | 0.000002 | |
| | | Base | Final taxonomy | 0.6673 | 0.003363 | 0.8907 | 0.000002 | |
| | Occurences | | Final taxonomy, Mid | 0.6547 | 0.004344 | No corrections | | |
| | Occurences | | Final taxonomy, Base | 0.6391 | 0.005747 | | | |

Coefficient results are calculated using Tables 2 and 3. Table 2 lists the number of **GPRs** in a polarity zone (column 2e), the **Duration Myr** (column 2d), and the **Total distribution** of all genera, using **Proportional dating** (column 2g), **Mid**-point (2i), and **Basal** dating (2h) of geologic stages. Correlation coefficients are calculated by comparing **Reversals perMyr** (Table 2f) to **20G genera** (Table 3, columns b to h) or **CRC genera** (Table 3, columns k to q) divided by the **Total Distribution** (Table 2, columns g to i) within **Polarity Zones** (Table 2, columns a and b). **Occurrences** are calculated using columns 2j and 2k. The **Corrected dating** spreadsheet of 1809 genera was an improvement by using the "Stratcomments" column in paleobiology.org.

**Individual Paleozoic polarity reversals** (reds are high polarity zones; blues are low polarity zones).

HPZ-17 (Guadalupian to Lopingian, Upper Permian): 252.46[4], 252.83[4], 253.0[4], 253.36[4], 253.72[4], 254.11[4], 254.35[4], 255.21[4], 257.20[4], 257.98[4], 258.18[4], 258.82[4], 259.7[4], 264.10[4], 264.42[4], 264.86[4], 266.07[4], 266.63[3], 267.63[3], 268.69[3], 270.0[3].

LPZ-16 (Kiaman Superchron, Upper Carboniferous to Lower Permian): 286.3, 297.3, 299.1, 299.3, 300.4, 300.8, 304.4, 308.7, 310.7, 311.75.

HPZ-15 (Upper Bashkirian): 316.2[5], 317.0, 318.6[4], 318.7[4], 318.8[4].

LPZ-14 (Upper Serpukhovian to Lower Bashkirian): 319.45, 322.7, 324.3, 326.92[4], 327.43[4].

HPZ-13 (Middle Viséan to Lower Serpukhovian, Carboniferous): 328.3, 328.65, 330.6, 331.3, 331.8, 331.9, 332.2, 332.3, 333.2, 333.35, 334.05, 334.25, 334.75, 334.9, 335.2, 335.7, 336.6, 336.8, 337.3, 337.5.

LPZ-12 (Romer's Gap, Early Tournaisian to Middle Viséan, Carboniferous): 343.0, 343.7, 344.3, 346.0, 347.45, 352.35.

HPZ-11 (Givetian to Famennian, Upper Devonian, plus Early Tournaisian): 356.7, 356.85, 357.6, 357.75, 358.4, 358.75, 360[1], 363.6[1], 364.7[1], 365.2[1], 367.7[1], 370.4[1], 371.5[1], 372.8[1], 373.3[1], 373.8[1], 375[1], 376.1[1], 377.3[1], 378.3[1], 378.65[1], 378.9[1], 379.3[1], 380.3[1], 381.6, 382.5[2], 383.1[2], 384.3[2], 386.4[2], 387.1[2], 387.7[2].

LPZ-10 (Middle Lochkovian to Eifelian, Lower Devonian): 393.3, 400.24, 400.76, 401.6[2], 402.5[2].

HPZ-9 (Ludlow to Pridoli Stages, Upper Silurian; Lower Lochkovian): 416.7, 418.2, 418.9, 419, 419.4, 419.9, 420.4, 420.9, 421.4, 421.9, 422.4, 422.9, 423.4, 423.9, 424.4, 424.9, 425.4, 425.9, 426.4, 426.9, 427.4.

HPZ-8 (Wenlock Stage, Middle Silurian): None.

HPZ-7 (Llandovery, Lower Silurian): 433.5, 433.8, 434.3, 434.8, 435.3, 435.8, 436.3, 436.8, 437.3, 437.8, 438.3, 438.8, 439.3, 439.8, 440.3, 440.8, 441.3, 441.8, 442.3, 442.8, 443.3, 443.8.

LPZ-6 (Middle Katian to Hirnantian, Ordovician): 448.9, 450.7.

HPZ-5 (Darriwilian to Lower Katian): 452.2, 452.34, 453, 453.6, 454.0[4], 454.73[4], 457.26[4], 457.7[4], 458.26[4], 459.19[4], 459.68[4], 461.21[4], 461.73[4], 462.11[4], 462.32[4], 462.76[4], 463.56[4], 464.6[4], 466.0[4], 466.8[4].

LPZ-4 (Moyero Superchron, Upper Tremadocian to Lower Darriwilian): 479.95, 480.1.

HPZ-3 (Cambrian Age 10 to Lower Tremadocian): 482.2, 482.7, 482.9, 484.35, 484.6, 484.8, 485.3, 485.9, 486.75, 486.95, 487.1, 487.2, 487.3, 487.8, 488.1[4], 490.05[4], 490.2[4].

LPZ-2 (Paibian to Upper Jiangshanian): 492[4], 492.2[4], 495[4].

HPZ-1 (Lower Cambrian): 497[4], 497.4, 497.55, 497.7, 497.85, 498.0, 498.1, 498.2, 498.3, 498.75, 498.95, 499.0, 499.15, 499.45, 499.6, 499.68, 499.75, 499.83, 499.9, 500.65, 500.75, 500.8, 501.1, 501.25, 501.45, 501.55, 501.65, 501.75, 501.8, 502.1, 502.2, 502.35, 502.8, 503.13, 503.6, 503.75, 504.1, 504.75, 505.3, 505.55, 506.7, 507.2, 508.9, 509.2, 509.52, 509.7, 510.17, 510.32, 510.6, 510.8, 511.72, 511.95, 512.05, 512.25, 512.4, 512.9, 513.4, 513.9, 514.4, 514.9, 515.4, 515.9, 516.18, 516.35, 517, 517.5, 517.6, 517.75, 517.85, 518.25, 518.35, 518.6, 518.64, 518.7, 518.85, 519.25, 519.25, 519.4, 519.55. 519.7, 520.2, 520.35, 520.6, 520.75, 520.85, 520.95.

Superscripts: 1 is for Ogg (2016); 2 is for Hansma (2015); 3 is for Lanci (2013); 4 is for Hounslow (2016); 5 is for Opdyke (2014). Polarity reversals without superscripts are from Gradstein (2012).

## References

Anderson, J.S., Smithson, T., Mansky C.F. & Clack, J. A. (2015) Diverse Tetrapod Fauna at the Base of Romer's Gap'. PLoS One. doi: 10.1371/journa.pone.0125446.

Benton M.J., Ruta M, Dunhill A.M., Sakamoto M. (2013) The first half of tetrapod evolution, sampling proxies, and fossil record quality. *Palaeogeography, Palaeoclimatology, Palaeoecology* Vol. **372**, 18-41.

Benton, M.J. (2015) *Vertebrate Palaeontology*, Fourth Edition. Wiley.

Clack, J.E., et al. (2016) Phylogenetic and environmental context of a Tournaisian tetrapod fauna. Nature Ecol & Evol.

Clack, J.A. (2012) *Gaining Ground, The Origin and Evolution of Tetrapods* Indiana University Press.

Coates, M.J, Ruta, M. Freidman, M. (2008) Ever Since Owen: Changing Perspectives on the Early Evolution of Tetrapods. *Annu. Rev. Evol. Sys.* **39**, 571-592.

Courtillow, V., Olson, P. (2007) Mantle plumes link magnetic superchrons to phanerozoic mass depletion events. *Earth and Planetary Science Letters* **260**, 495-504.

Crutzen, P.J., Isaksen I.S., Reid, G.C. (1975) Solar proton events: Stratospheric sources of nitric oxide. *Science* **189**, 457–459.

Glassmeier, K.H., Vogt J. (2010) Magnetic Polarity Transition and Biospheric effect, Historical Perspective and Current Developments. *Space Sci Rev* **155,** 387-400.

Gradstein F.M., Ogg, J.G., Schmitz, M.D., Ogg, G.M. (2012) *The Geologic Time Scale* Elsevier.

Harrison, C.G.A., Prospero, J.M. (1974) Reversals of the Earth's magnetic field and climate changes. *Nature* **250**, 563-65.

Huang, C. et al. (2017) The Contribution of Geomagnetic Activity to Polar Ozone Changes in the Upper Atmosphere *Advances in Meteorology* Volume 2017.

Hansma, J. *et al*. (2015) Late Devonian carbonate magnetostratigraphy from the Oscar and Horse Spring Ranges, Lennard Shelf, Canning Basin, western Australia. *Earth and Planetary Science Letters* **409**: 232–242.

Hounslow, Mark W. (2016) Geomagnetic reversal rates following Palaeozoic superchrons have a fast restart mechanism. *Nature Communications* **7**. doi:10.1038/ncomms12507.

Kemp, T.S. (2005) *The Origin and Evolution of Mammals*.

Kemp, T.S. (2006) The origin and early radiation of the therapsid mammal-like reptiles: a palaeobiological hypothesis. *J. Evol. Biol.*, Volume **19**, 1231–1247.

Kemp, T.S. (2009) *Phylogenetic interrelationships and pattern of evolution of the therapsids: testing for polytomy.*

Kemp, T.S. (2012) The Origin and Radiation of Therapsids, in *Forerunners of Mammals* Chapter 1, edited by Chinsamy-Turan.

Kryza, R, et al. (2011) A SIMS zircon age for a biostratigraphically dated Upper Viséan (Asbian) bentonite in the Central-European Variscides (Bardo Unit, Polish Sudetes). International Journal of Earth Science Vol 11, Issue 6, pp 1227-1235.

Lanci, L., Tohver, E., Wilson, A., Flint, S. (2013) Upper Permian magnetic stratigraphy of the lower Beaufort Group, Karoo Basin. *Earth and Planetary Science Letters* **375**: 123–134.

Laurin, M. (2004) The Evolution of Body Size, Cope's Rule and the Origin of Amniotes. Syst. Biol. **53**, 594-622.

Liu, J., Rubidge,B, Li, J. (2009)New basal synapsid supports Laurasian origin for therapsids. *Acta Palaeontologica Polonica* 54, 3.

Liu, J. (2001) The most primitive lower tetrapod fauna in China Sci. China Ser. D-Earth Sci.

Liu, J., Rubidge,B, Li, J. (2009) New basal synapsid supports Laurasian origin for therapsids. *Acta Palaeontologica Polonica* 54, 3.

Lu, J, et al. (2012) The earliest known stem-tetrapod from the Lower Devonian of China *Nat Comun* 3:1160.

Lucas, S.G. (2015) Thinopus and a Critical Review of Devonian Tetrapod Footprints. Ichnos Vol 22.

Liboff, A.R. (2013) Weak-field ELF magnetic interactions: Implications for biological change during paleomagnetic reversals. *Electromagn. Biol. Med.* Volume **32**.

McHargue, L.R. *et al*. (2000) Geomagnetic modulation of the late Pleistocene cosmic-ray flux as determined by $^{10}$Be from Blake Outer Ridge marine sediments. *Nucl. Instrum. Methods Phys. Res. B* **172**, 555–561.

Ogg, J.G., Ogg G.M. (2016) *A Concise Geologic Time Scale* Elsevier.

Opdyke, N.D., Giles, P.S., Uttin, J. (2014) Magnetic polarity stratigraphy and palynostratigraphy of the Mississippian-Pennsylvanian boundary interval in eastern North America and the age of the beginning of the Kiaman. *GSA Bulletin* **126**, 1068-1083.

Paton, R.L.,Smithson, T.R., Clack, J.A. (1999) An amniote-like skeleton from the Early Carboniferous of Scotland, Nature 398, 508-513.

Pechersky D.M., Lyubushin A.A., Sharonova Z.V. (2012) On the Coherence between Changes in Biota and Geomagnetic Reversals in the Phanerozoic. *Russian Academy of Sciences*, Vol. **48** 44-62.

Peters, S.E. and Foote, M. (2001) Biodiversity in the Phanerozoic: a reinterpretation. *Paleobiology* **27**, 583-601.

Raisbeck, G. M., Yiou, F., Cattani, O., Jouzel, J. (2006) $^{10}$Be evidence for the Matuyama–Brunhes geomagnetic reversal in the EPICA Dome C ice core". *Nature* **444**: 82–84.

Sansom R.S., Randle, E., Donoghue, P.C.J. (2014) Discriminating signal from noise in the fossil record of early vertebrates reveals cryptic evolutionary history. Biol. Sci. **282**.

Sepkoski, J.J. (2002) A compendium of fossil marine animal genera. *Bulletins of American paleontology*. No. **363**.

Smith, M.P., (2007) The Cambrian origin of vertebrates, in *Major Events in Early Vertebrate Evolution*, *Palaeontology, phylogeny, genetics and development*. Edited by Per Erik Ahlberg..

PeerJ Preprints | https://doi.org/10.7287/peerj.preprints.26490v1 | CC BY 4.0 Open Access | rec: 7 Feb 2018, publ: 7 Feb 2018

Uffen R.J., (1963) Influence of the Earth's core on the origin and evolution of life. *Nature* **198**, 143–144.

VanTuinen, M., Hadly, E.A. (2004) Error in estimation of rate and time inferred from the early amniote fossil record and avian molecular clocks. *J Mol Evol* 59:267-276.

Wei, Y. *et al*. (2014) Oxygen escape from the Earth during geomagnetic reversals: Implications to mass extinction. *Earth and Planetary Science Letters* **394**, 94-98.

Zhao, W.J., Zhu, M. (2010) Siluro-Devonian vertebrate biostratigraphy and biogeography of China. Palaeoworld 19, 4-26. Doi:10.1016/j.palwor.2009.11.007

Zhu, M. (1998) Early Silurian sinacanths (Chondrichthyes) from China. *Palaeontology* **41**, 157-171.

Zhu, M. *et al*. (2009) The oldest articulated osteichthyan reveals mosaic gnathostome characters. *Nature* **458**, 469-474.